Neurobiology of Disease 141 (2020) 104879

Contents lists available at ScienceDirect

Neurobiology of Disease

journal homepage: www.elsevier.com/locate/ynbdi

Transcriptomic and proteomic profiling of glial versus neuronal *Dube3a* overexpression reveals common molecular changes in gliopathic epilepsies

Kevin A. Hope[a,b,1], Daniel Johnson[c], P. Winston Miller[c], Daniel Lopez-Ferrer[d], David Kakhniashvili[e], Lawrence T. Reiter[a,f,g,*]

[a] Department of Neurology, UTHSC, Memphis, TN, United States of America
[b] Integrated Biomedical Science Program, UTHSC, Memphis, TN, United States of America
[c] Molecular Bioinformatics Core, UTHSC, Memphis, TN, United States of America
[d] Thermo Fisher Scientific, UTHSC, 180 Oyster Point Blvd, South San Francisco, CA, United States of America
[e] Proteomics and Metabolomics Core, UTHSC, Memphis, TN, United States of America
[f] Department of Pediatrics, UTHSC, Memphis, TN, United States of America
[g] Department of Anatomy and Neurobiology, UTHSC, Memphis, TN, United States of America

ARTICLE INFO

Keywords:
Epilepsy
Seizure
Drosophila
Glia
Glutathione S-transferase
Dup15q
Gliopathic

ABSTRACT

Epilepsy affects millions of individuals worldwide and many cases are pharmacoresistant. Duplication 15q syndrome (Dup15q) is a genetic disorder caused by duplications of the 15q11.2-q13.1 region. Phenotypes include a high rate of pharmacoresistant epilepsy. We developed a Dup15q model in *Drosophila melanogaster* that recapitulates seizures in Dup15q by over-expressing fly *Dube3a* or human UBE3A in glial cells, but not neurons, implicating glia in the Dup15q epilepsy phenotype. We compared *Dube3a* overexpression in glia (*repo* > *Dube3a*) versus neurons (*elav* > *Dube3a*) using transcriptomics and proteomics of whole fly head extracts. We identified 851 transcripts differentially regulated in *repo* > *Dube3a*, including an upregulation of glutathione S-transferase (GST) genes that occurred cell autonomously within glial cells. We reliably measured approximately 2,500 proteins by proteomics, most of which were also quantified at the transcript level. Combined transcriptomic and proteomic analysis revealed an enrichment of 21 synaptic transmission genes downregulated at the transcript and protein in *repo* > *Dube3a* indicating synaptic proteins change in a cell non-autonomous manner in *repo* > *Dube3a* flies. We identified 6 additional glia originating bang-sensitive seizure lines and found upregulation of GSTs in 4 out of these 6 lines. These data suggest GST upregulation is common among gliopathic seizures and may ultimately provide insight for treating epilepsy.

1. Introduction

Epilepsy affects approximately 1% of humans worldwide in their lifetime (Fiest et al., 2017). Despite advances in epilepsy treatment, uncontrolled epilepsy remains common and approximately 30-50% of people with epilepsy ultimately develop treatment resistant seizures (Kwan and Brodie, 2000; LaPenna and Tormoehlen, 2017; Golyala and Kwan, 2017). Investigating the mechanism by which treatment resistant seizures occur, and identifying molecular commonalities among different genetic causes of seizures, can help fill the gap in our knowledge about why epilepsy is refractory to many current treatments.

One genetic disorder with a high rate of treatment resistant epilepsy that may serve as an entry point into investigating treatment resistant seizures is Duplication 15q syndrome, or Dup15q (Finucane et al., 2016). Dup15q results from maternally derived duplications of chromosome 15q11.2-q13.1 and individuals with Dup15q harbor 1 to 6 extra copies of this region. A retrospective survey on seizure in Dup15q indicated that seizure severity was positively correlated with 15q11.2-q13.1 copy number as 25% of interstitial duplications (1 extra copy), 64% of isodicentric duplications (2 extra copies), and 100% of complex duplications (up to 6 extra copies) presented with seizures. As low as 25% of individuals with isodicentric Dup15q had a > 90% reduction in seizures after the first medication, and seizures were refractory in roughly 75% of epileptic individuals (Conant et al., 2014).

The majority of Dup15q research has focused on neuronal

* Corresponding author at: Department of Neurology, The University of Tennessee Health Science Center, 855 Monroe Ave., Link 431, Memphis, TN 38163, United States of America.
E-mail addresses: khope@genetics.utah.edu (K.A. Hope), lreiter@uthsc.edu (L.T. Reiter).
[1] Current Address: Department of Human Genetics, University of Utah School of Medicine, Salt Lake City, UT

https://doi.org/10.1016/j.nbd.2020.104879
Received 16 October 2019; Received in revised form 4 April 2020; Accepted 23 April 2020
Available online 25 April 2020

overexpression of the E3 ubiquitin ligase *UBE3A*. Due to the complex imprinted regulation in neurons at the 15q11.2-q13.1 locus, *UBE3A* is only expressed from the maternal allele in mature mammalian neurons (LaSalle et al., 2015). Dup15q characteristics other than seizures have been successfully recapitulated in mouse models, such as social abnormalities and behavioral inflexibility (Nakatani et al., 2009), social interaction deficits (Smith et al., 2011), and seizure-induced decreased sociability (Krishnan et al., 2017). However, modeling seizure susceptibility itself has been difficult to do in rodent models. A recent mouse model restricting *Ube3a* overexpression to excitatory neurons caused slightly reduced threshold to pharmacologically induced seizures, yet spontaneous seizure behavior was not described (Copping et al., 2017).

To develop a seizure model of Dup15q, we turned to *Drosophila melanogaster* and the powerful GAL4/UAS system (Brand and Perrimon, 1993; Duffy, 2002). This new Dup15q model in flies recapitulates the seizure phenotype when *Dube3a* (the fly *UBE3A* homolog) or human *UBE3A* is overexpressed in glial cells (*repo* > *Dube3a*), not neurons (*elav* > *Dube3a*), implicating glia in the etiology of Dup15q seizures (Hope et al., 2017). Glial cells biallelically express *Ube3a* in mice (Yamasaki et al., 2003; Dindot et al., 2008; Judson et al., 2014; Grier et al., 2015), and GFAP positive astrocytes in the human brain similarly express *UBE3A* (Burette et al., 2018). Based on these observations, we propose that Dup15q individuals have elevated levels of UBE3A in glia and neurons. The contribution of glial cells, particularly astrocytes, to epilepsy is becoming more apparent (Coulter and Steinhauser, 2015), and increased UBE3A levels in human glia may cause the underlying molecular deficits that lead to seizures in Dup15q.

Previously, we identified reduced levels of the Na^+/K^+ exchanger ATPα in our glial *Dube3a* overexpression seizure model that appeared to drive a large portion, but not all, of the seizure phenotype (Hope et al., 2017). As such, further characterization of *repo* > *Dube3a* seizure sensitive flies was needed. In this study we employed whole transcriptome analysis through RNA-sequencing and whole proteome analysis through liquid chromatography coupled to high-resolution mass spectrometry of whole fly head extracts in order to identify the underlying changes in glial or neuronal *Dube3a* overexpression. By combining both transcript and protein profiling, we were able to identify genes that were altered at either the transcript level, the protein level, or both the transcript and protein level based on *Dube3a* cell-type specific overexpression.

2. Methods

2.1. Fly stocks

Flies were reared on standard corn meal media (Bloomington Stock Center) and maintained on a 12-hour light/dark cycle at 25°C. *repo-GAL4* was obtained from the Bloomington Drosophila Stock Center (BDSC # 7415, RRID:BDSC_7415), *elav-GAL4* was provided by Dr. Hugo Bellen (Baylor College of Medicine), and *uas-Dube3a* was described previously (Reiter et al., 2006). The *GSTD1-LacZ* reporter line was provided by Mel Feany and Dirk Bohmann and has been described previously (Sykiotis and Bohmann, 2008). See Supplemental Table 1 for a complete list of stocks.

2.2. RNA sequencing

RNA was isolated from control (*uas-Dube3a* alone), glial *Dube3a* overexpression (*repo* > *Dube3a*), or neuronal overexpression of *Dube3a* (*elav* > *Dube3a*) flies by removing 15-25 fly heads per genotype and homogenizing in TRI Reagent (Applied Biosystems). Total RNA was extracted with Directzol RNA MiniPrep Plus (Zymo Research Corp) according to the manufacturer's instructions which included a DNAse treatment step. Purity and concentration was verified using NanoDrop spectrophotometer (ThermoFisher Scientific), and integrity was confirmed using a Bioanalyzer (Agilent). Each genotype was run in triplicate. RNAseq was performed by PGM sequencing at the UTHSC Molecular Resource Center (MRC). Each RNA sample was converted to ion torrent sequencing libraries and run on 318v2 chips using an Ion Torrent Proton sequencer. All groups and replicates were run simultaneously to eliminate chip-to-chip variability.

2.3. RNAseq analysis

At least 35M unmapped reads we available per replicate sample for three groups and three replicates (1) *uas-Dube3a*, (2) *repo* > *Dube3a*, (3) *elav* > *Dube3a*. RNAseq alignments and analysis was performed using a local Slipstream appliance running a GALAXY installation. All FASTQ files were gathered from the sequencer. Quality assurance was performed using FASTQC. All reads were trimmed to remove any nucleotide that fails a phred score $\leq$ Q20. The trimmed FASTQ files were aligned to the reference library using RNA STAR. Once aligned, the SAM files were collected and mined for read count information of each gene present in the reference file. Read counts were normalized using Transcripts per Million (TPM) method across the entire experiment. The resulting data was analyzed with DeSeq2. All genes that failed to yield at least a 1.5 fold change and a p-value greater than 0.05 were removed. Benjamini and Hochberg false discovery rate was performed on the trimmed gene list. All genes that failed to yield a false discovery rate $\leq$ 0.05 were removed. The final significant differential gene list were loaded into R for visualization.

2.4. Quantitative proteomics

Protein was extracted from fly heads by homogenizing 30-40 fly heads of each genotype in RIPA buffer plus complete Protease Inhibitor Cocktail (Roche). Lysates were de-salted and immobilized using a Filter Aided Sample Preparation (FASP) column followed by trypsin digestion and Tandem Mass Tag (TMT) labeling as described elsewhere (Jiang et al., 2017). All groups were labeled at once to avoid variance in labeling reactions. The labeled digested peptides were then were analyzed by LC-MS/MS using an EASY-nLC 1000 UPLC system (Thermo Fisher Scientific San Jose, CA) with a 50 cm EASY-Spray Column coupled to an Orbitrap Fusion Lumos (Thermo Fisher Scientific, San Jose, CA) mass spectrometer. Separations were carried out using a 210 min gradient at a flow rate of 300 nL/min.

Post-acquisition analysis of raw MS data was performed with mass informatics platform Proteome Discoverer 2.0 and searched with the SEQUEST HT search engine. Precursor mass tolerance was set to 10 ppm. Fragment ion tolerance was 0.02 Da when using the Orbitrap analyzer and 0.6 Da when using the ion trap analyzer. Carbamidomethylation on cysteine (+57.021 Da) and TMT6 tags on N termini as well as lysine (+229.163 Da) were set as static modifications. Dynamic modifications included oxidation on methionine (+15.995 Da). Data were searched against a UniProt *Drosophila melanogaster* database. Peptide identification data was used for identification and quantification of corresponding parent proteins; Peptide abundance was calculated using signal to noise (S/N) values from corrected reporter ion abundances based on the manufacturer's data sheets. S/N values where then log transformed and roll up at the protein level by summing the values for all the peptides to represent protein abundance. An ANOVA test was then performed to determine statistically relevant differences. For statistical validation of results, the FDR (False Discovery Rate) was determined and differences were considered statistically significant if FDR $\leq$ 0.05.

2.5. Combined RNAseq and Proteomic Analysis

RNAseq and proteomics data were combined into a single analysis by selecting proteins that were significantly differentially expressed that were also detected at the transcript level. Protein abundance ratios

were used to calculate the protein Log_2 fold change and FPKM were used to calculate transcript Log_2 fold change.

2.6. Quantitative western blot analysis

Protein was extracted from 30-40 fly heads by homogenization in RIPA buffer plus Complete Protease Inhibitor Cocktail (Roche). Samples were spun at 10,000 x g to remove exoskeleton. 20 μg of protein was loaded into 1.5 mm NuPAGE Bis-Tris 4-12% gels (Invitrogen) and subsequently transferred to PVDF membranes (Millipore). Membranes were blocked with Odyssey Blocking Buffer (Li-Cor cat # 927-50000). The following primary antibodies were diluted in Odyssey Blocking Buffer with 0.2% tween-20: α-GAPDH (1:5000, Abcam ab157156), α-futsch (1:100, DSHB, 22C10, RRID:AB_528403), α-synapsin (1:100, DSHB, 3C11, RRID:AB_2313867), α-Sap47 (1:100, DSHB, nc46, RRID:AB_2617213), α-Syx1a (1:100, DSHB, 8C3, RRID:AB_528484), and α-Nwk (1:1000, gift from J. Troy Littleton (Picowar Institute at MIT)). The following infrared secondary antibodies were diluted at 1:15,000 in Odyssey Blocking Buffer with 0.2% tween-20 and 0.01% SDS: α-goat (Licor Cat# 925-68074, RRID:AB_2650427), α-mouse (Licor Cat# 926-32212, RRID:AB_621847), and α-rabbit (Licor Cat# 925-32211, RRID:AB_2651127). Blots were imaged using an Odyssey Infrared Imaging System (Licor) and analyzed using Image Studio Lite (Licor) normalizing experimental bands to GAPDH as the loading control for calculating normalized adjusted relative signal intensities. All samples were run $\geq$ 3 times to perform statistical analysis, and differences were considered statistically significant if $p \leq 0.05$.

2.7. Seizure susceptibility assays

Seizure assays were performed as previously described (Hope et al., 2017). Briefly, flies were collected on the day of eclosure under CO_2 anesthesia and aged 3-5 days. On the day of testing flies were gently transferred by mouth pipette to empty vials. Flies were subjected to mechanical stress ("bang") by vortexing for 10 s on a standard laboratory vortexer (LabNet) at full speed. Recovery time was recorded for each fly as measured by time until the fly righted itself and was able to walk or groom and no longer displayed paralysis or uncontrolled muscle movements. To detect seizure sensitive flies, all experimental groups were compared to the control *repo > 36303-emptyvector-RNAi* by one-way ANOVA followed by Dunnett's multiple comparison test. Groups were considered statistically significant if $p \leq 0.05$.

2.8. Microarray analysis

Total RNA was isolated from control (*repo > 36303-emptyvector-RNAi*) and gliopathic seizure lines by removing 15-25 fly heads per genotype and homogenizing in TRI Reagent (Applied Biosystems) and followed by RNA purification with Directzol RNA MiniPrep Plus (Zymo Research Corp) according to the manufacturer's instructions. Purity and concentration was verified using NanoDrop spectrophotometer (ThermoFisher Scientific) and Qubit (ThermoFisher Scientific). RNA integrity was measured using a Bioanalyzer (Agilent). mRNA from the gliopathic seizure flies was pooled into a single group by adding equal amounts of mRNA from each sample. Samples were run on a GeneChip Drosophila Gene 1.0 ST Array (ThermoFisher Scientific, #902155).

Comma-separated value (CSV) files were retrieved from UTHSC Molecular Resource Center after normalization performed by Affymetrix Expression Console. Quality assurance was checked against reference probes to ensure quality of data. Gene names, accession numbers, and expression were mined from each text file for each sample. All non-annotated information was removed from the file leaving only annotated gene expression. A Welsh *t*-test was run for pairwise interactions in order to obtain p-values for significance. Only genes with a p-value $\leq$ 0.05 were considered significant. The mean, variance, standard deviation, and fold change were calculated for each pairwise comparison. Benjamini Hochberg false discovery rate method was applied in order to obtain the adjusted p-value for each gene. Only genes with an adjusted p-value $\leq$ 0.05 were considered significant.

2.9. Quantitative real-time polymerase chain reaction (qRT-PCR)

mRNA was converted to cDNA using a Transcriptor First Strand cDNA Synthesis Kit (Roche, 04379012001) according to the manufacturer's instructions. Briefly, 500 ng of total mRNA was used per genotype with random hexamer primers for cDNA synthesis. Probes were selected and primers were designed using the Universal Probe Library Assay Design Center software (Roche). For a complete list of probes and primers see Supplemental Table 2. All assays were performed in triplicate for each cDNA sample. Cycling conditions of the Roche LC480 were: 95°C for 5 m followed by 40 cycles of 95°C for 10 s, 60°C for 30 s, and 72°C for 10 s during which fluorescence was measured. Crossing point (Cp) values were calculated for each sample using the absolute quantification algorithm (Roche), and average Cp values for three technical replicates were calculated. The average Cp values were normalized to *TATA-binding protein* (*tbp*). Log_2 fold change was calculated by first finding the ΔCp for each sample, comparing experimental groups to the control group to calculate ΔΔCp, calculating fold change with the equation $Fc = (2)^{-\Delta\Delta Cp}$, and finally making the Log_2 transformation.

2.10. Immunohistochemistry and image acquisition

Immunohistochemistry was performed as described previously (Hope et al., 2017). Briefly, flies were anesthetized with CO_2 and brains were dissected in phosphate buffered saline (PBS) and fixed with 4% formaldehyde for 1 hour. Brains were blocked and permeabilized with 5% bovine serum albumin and 0.1% Triton X-100. Primary antibodies used were rabbit α-βGal (1:100, Thermofisher Scientific 14-6773-81, RRID:AB_468331) and mouse α-repo (1:100, DSHB 8D12, RRID_AB:528448), incubated overnight at 4°C in the same blocking solution. Secondary antibodies used were donkey α-rabbit 594 (1:500, Thermofisher Scientific A21207, RRID:AB_141637) and goat α-mouse 488 (1:500, Thermofisher Scientific A11029, RRID:AB_2534088) and were incubated for 1 hour at room temperature. Slides were mounted with Fluoromount-G mounting media (SouthernBiotech, 0100-20) and sealed with clear nail polish.

Confocal images were acquired using a Zeiss 710 laser scanning confocal microscope (Zeiss) located in the UTHSC Neuroscience Institute Imaging Core. Images were captured at 1024x1024 resolution with a 63X objective lens at 1 μM Z-section thickness. Detector gain and offset were optimized for the control group and settings were kept consistent across treatment groups to allow for comparisons between groups. Images were analyzed using Fiji (Schindelin et al., 2012) by selecting the area of interest and calculating the integrated density using the measure tool.

2.11. Feeding flies picrotoxin (PTX)

A 50 mM stock solution of PTX (Acros Organics) was made in DMSO. Flies were fed 2.5 mM PTX in 5% sucrose (Sigma) with 1% green food color by placing flies in a vial containing a Kimwipe saturated with PTX feeding solution. Flies were left to feed for 24 hours, and consumption was confirmed by the presence of green dye in their abdomens. Control flies were fed DMSO alone.

2.12. Data analysis

Data analysis and statistical tests were performed using Prism 6.0 (GraphPad). To determine differences between multiple samples, one-way ANOVA was used with Tukey's multiple comparisons (α was set to 0.05). Heatmaps were generated using R-Studio and figures were

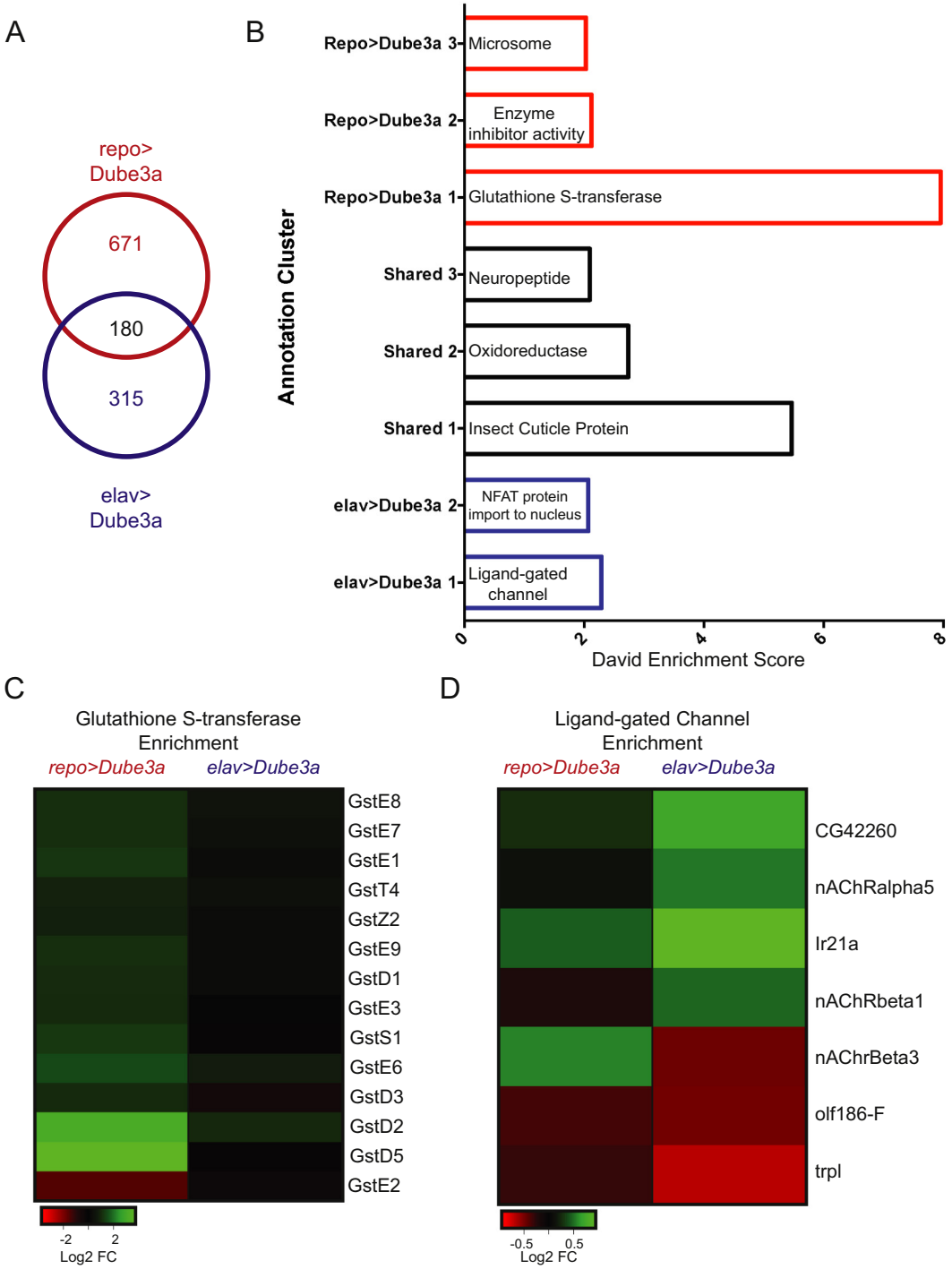

Fig. 1. Transcript profiling reveals an upregulation of GST genes in *repo > Dube3a* flies. A) Venn diagram of differentially expressed transcripts between *repo > Dube3a* and *elav > Dube3a* compared to *uas-Dube3a* controls. B) DAVID enrichment groups for differentially expressed transcripts in each portion of the Venn diagram. C) Heatmap indicating an upregulation of 13/14 GST genes in *repo > Dube3a*. This upregulation was not observed in neuronal *elav > Dube3a* overexpression. D) Heatmap illustrating the differential expression for the "ligand-gated channel" enrichment group observed in *elav > Dube3a*.

generated in Adobe Illustrator (Adobe).

3. Results

3.1. Transcriptomic profiling reveals an upregulation of glutathione S-transferases in repo > Dube3a fly heads

We previously demonstrated that *repo > Dube3a* flies overexpressing *Dube3a* in all glial cells display a severe bang-sensitive seizure phenotype, while *elav > Dube3a* flies expressing *Dube3a* in all neurons do not (Hope et al., 2017). In order to investigate gene expression changes in these animals at the transcript level we performed RNAseq using RNA extracted from whole fly heads in control *uas-Dube3a* alone, glial *Dube3a* overexpression *repo > Dube3a*, and neuronal *Dube3a* overexpression *elav > Dube3a* flies. We reliably identified and quantified transcripts from approximately 11,000 genes across all

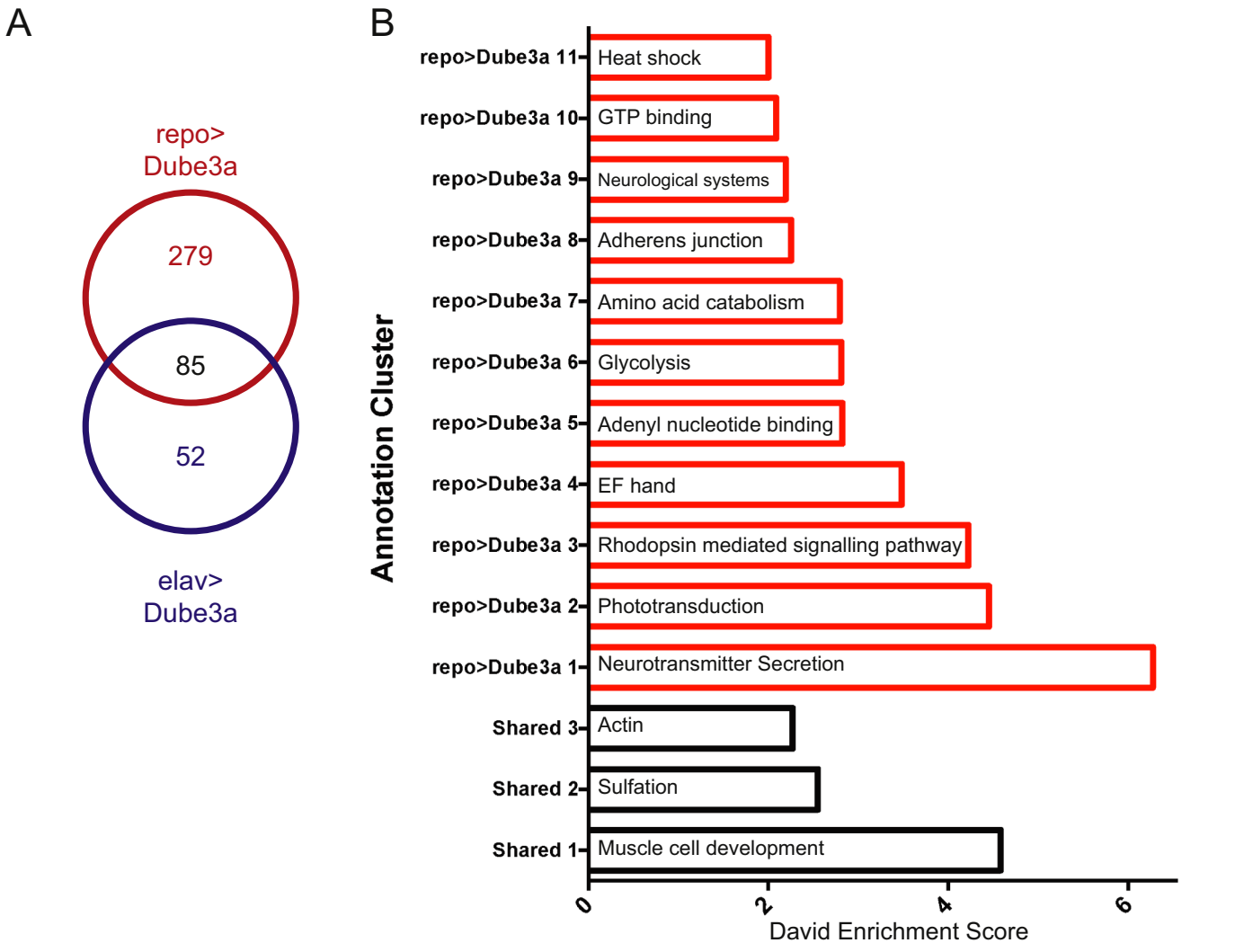

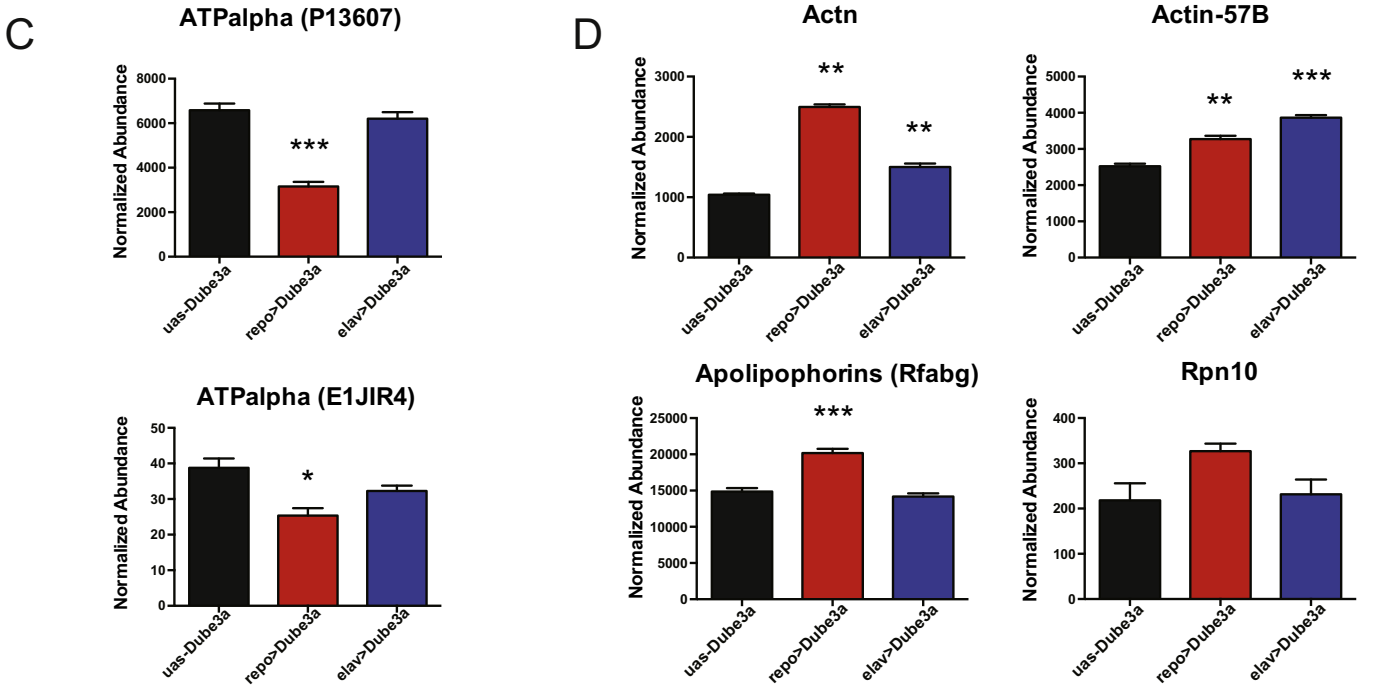

(caption on next page)

Fig. 2. Proteomic profiling reveals differential expression of neurotransmitter secretion proteins in *repo > Dube3a* flies. A) Venn diagram of differentially expressed proteins between *repo > Dube3a* and *elav > Dube3a*. B) DAVID enrichment groups with an enrichment score greater than 2 for differentially expressed proteins for each portion of the Venn diagram. C) Normalized abundance ratios for the two detected isoforms of the Na+/K+ ATPase ATPα following overexpression of *Dube3a* in glia or neurons compared to controls indicates downregulation of both isoforms only in *repo > Dube3a* fly heads. D) Normalized abundance ratios for proteins previously reported to be regulated in a *Dube3a* dependent manner. Error bars represent S.E.M, and * = FDR ≤ 0.05, ** = FDR ≤ 0.01, and *** = FDR ≤ 0.005.

three groups. We found 851 differentially expressed genes in *repo > Dube3a* compared to *uas-Dube3a* controls and 495 differentially expressed genes in *elav > Dube3a* compared to controls (p-adjusted ≤ 0.05). Of these differentially expressed transcripts, 180 were shared between *repo > Dube3a* and *elav > Dube3a* (Fig. 1A, Supplemental Table 3).

To identify biological enrichments within each portion of the Venn diagram, we utilized the Database for Annotation, Visualization, and Integrated Discovery (Huang Da et al., 2009a; Huang et al., 2009b), and plotted DAVID analysis enrichment groups with an enrichment score (ES) greater than 2 for each group (Fig. 1B). In the 180 differentially expressed genes shared between *repo > Dube3a* and *elav > Dube3a*, we observed an enrichment in "insect cuticle proteins" (ES = 5.46), "oxidoreductase" (ES = 2.73), and "neuropeptide" (ES = 2.09), (Fig. 1B). Within the 671 *repo > Dube3a* specific differentially expressed genes we found the strongest enrichment in "glutathione S-transferase" (ES = 7.96). For the 315 *elav > Dube3a* specific significantly differentially expressed transcripts we observed an enrichment in "ligand-gated channel activity" (ES = 2.29) and "positive regulation of NFAT protein import into nucleus" (ES = 2.07) (Fig. 1B, for all enrichment groups see Supplemental Table 3). We plotted the Log_2 fold change for GST enrichment observed in *repo > Dube3a* for *repo > Dube3a* and *elav > Dube3a* compared to controls and observed an upregulation of 13/14 GST genes and a downregulation of *GstE2* in *repo > Dube3a* that remained largely unchanged in *elav > Dube3a* (Fig. 1C). We also plotted the Log_2 fold change for the ligand-gated channel enrichment from *elav > Dube3a* for *repo > Dube3a* and *elav > Dube3a* compared to controls (Fig. 1D). These results indicate that overexpression of *Dube3a* in glial cells has a stronger impact on the global transcriptome compared to neuronal *Dube3a* overexpression. Additionally, overexpression of *Dube3a* in glia causes both seizures and an upregulation of GST genes.

3.2. Proteomic profiling reveals differential expression of neurotransmitter secretion proteins in repo > Dube3a fly heads

Next, we investigated global changes at the protein level using quantitative proteomics through mass spectrometry. We reliably identified and quantified approximately 2,500 proteins across each sample. 364 proteins were differentially expressed (FDR ≤ 0.05) in *repo > Dube3a* compared to control *uas-Dube3a*, and 137 were differentially expressed (FDR ≤ 0.05) in *elav > Dube3a* compared to *uas-Dube3a* flies. Of these differentially expressed proteins, 85 were shared between *repo > Dube3a* and *elav > Dube3a* (Fig. 2A, see Supplemental Table 4 for proteomics data). The 85 shared differentially expressed proteins were significantly enriched in three groups with an ES > 2.0; "muscle cell development" (ES = 4.58), "Sulfation" (ES = 2.55), and "Actin" (ES = 2.72) (Fig. 2B, Supplemental Table 4). The enrichment of the GO term "muscle cell development" was initially concerning, suggesting possible contamination in the protein prep. The proteins included in the enrichment group are *futsch, wupa, mf, up, act88f,* and *prm*, all of which were detected in proteomic analysis of adult Drosophila heads in previous studies (Aradska et al., 2015). Additionally, *futsch* is found at the neuromuscular junction (NMJ) causing *futsch* to be included in the GO term "muscle cell development", however *futsch* is known to be expressed from the neuronal side at the NMJ and is expressed widely throughout the central nervous system (Hummel et al., 2000), alleviating any concerns. The 279 *repo > Dube3a* specific differentially expressed proteins were significantly enriched in 11 groups with an ES > 2.0, the top two being "neurotransmitter secretion" (ES = 6.27) and "phototransduction" (ES = 4.45) (Fig. 2B, Supplemental Table 4). Within the 52 *elav > Dube3a* specific differentially expressed proteins, no enrichment group was observed with an ES > 2.0, however the top enrichment was "stress response" (ES = 1.96). Similar to our RNAseq data, these results suggest that overexpression of *Dube3a* in glia causes a larger change in the global proteomic landscape of the fly brain compared to overexpression of *Dube3a* in neurons. Additionally, we observed an enrichment in the GO term "neurotransmitter secretion" and "phototransduction" which are predominantly neuronal processes, suggesting cell non-autonomous effects of glial *Dube3a* overexpression in *repo > Dube3a* flies.

We previously reported downregulation of ATPα upon overexpression of *Dube3a* in glial cells (Hope et al., 2017) and that ATPα can be ubiquitinated by Dube3a (Jensen et al., 2013). We detected two peptides that mapped to two different isoforms of ATPα and we observed significantly reduced ATPα levels in the *repo > Dube3a* group for both ATPα accession P13607 (p ≤ 0.0005) and for ATPα accession E1JIR4 (p ≤ 0.01), however we did not observe significant reductions in either isoform of ATPα in *elav > Dube3a* flies (Fig. 2C). These results confirm our prior findings that elevated levels of Dube3a in glial cells results in reduced levels of ATPα protein (Hope et al., 2017). Additionally, we checked the levels of other proteins found to be influenced by Dube3a. Actin, Actin-57B, and apolipophorins were previously reported to be upregulated following elevated levels of Dube3a protein by our group (Jensen et al., 2013). Here we observed an upregulation of both Actin and Actin57B in both *repo > Dube3a* and *elav > Dube3a,* and apolipophorins was only upregulated in *repo > Dube3a* (Fig. 2D), confirming our previous proteomics results (Jensen et al., 2013). Rpn10 has been reported as a direct Ube3a substrate (Lee et al., 2014), however we detected no significant difference in Rpn10 levels in *elav > Dube3a* or *repo > Dube3a*, with levels slightly, but not significantly, increased in the *repo > Dube3a* group (Fig. 2D).

3.3. Comparison of the transcriptome and the proteome reveals downregulation of synaptic transmission proteins in repo > Dube3a fly heads

We compared the proteome and the transcriptome to determine whether expression changes at the protein level could be explained by changes at the transcript level. We selected all differentially expressed proteins that were also detected at the transcript level and mapped the Log_2 fold change of both the transcript and protein for *repo > Dube3a* compared to *uas-Dube3a* (Fig. 3A, Supplemental Table 5) and for *elav > Dube3a* compared to *uas-Dube3a* (Fig. 3B, Supplemental Table 6). Quadrants I, II, III, and IV represent genes upregulated at both the protein and transcript level, genes upregulated at the protein level but downregulated at the transcript level, genes downregulated at both the protein and transcript level, and genes downregulated at the protein level but upregulated at the transcript level, respectively.

Of the 160 proteins upregulated in *repo > Dube3a*, 130 (81.3%) were also differentially expressed at the transcript level. In quadrant I, 81 of 130 upregulated proteins (62.3%) were also upregulated at the transcript level. In quadrant II, 49 of 130 upregulated proteins (37.7%) were downregulated at the transcript level. Of the 204 downregulated proteins in *repo > Dube3a*, 185 (90.1%) were also differentially expressed at the transcript level. In quadrant III, 112 of 185 downregulated proteins (60.5%) were also downregulated at the transcript. In quadrant IV, 73 of 185 downregulated proteins (39.5%) were

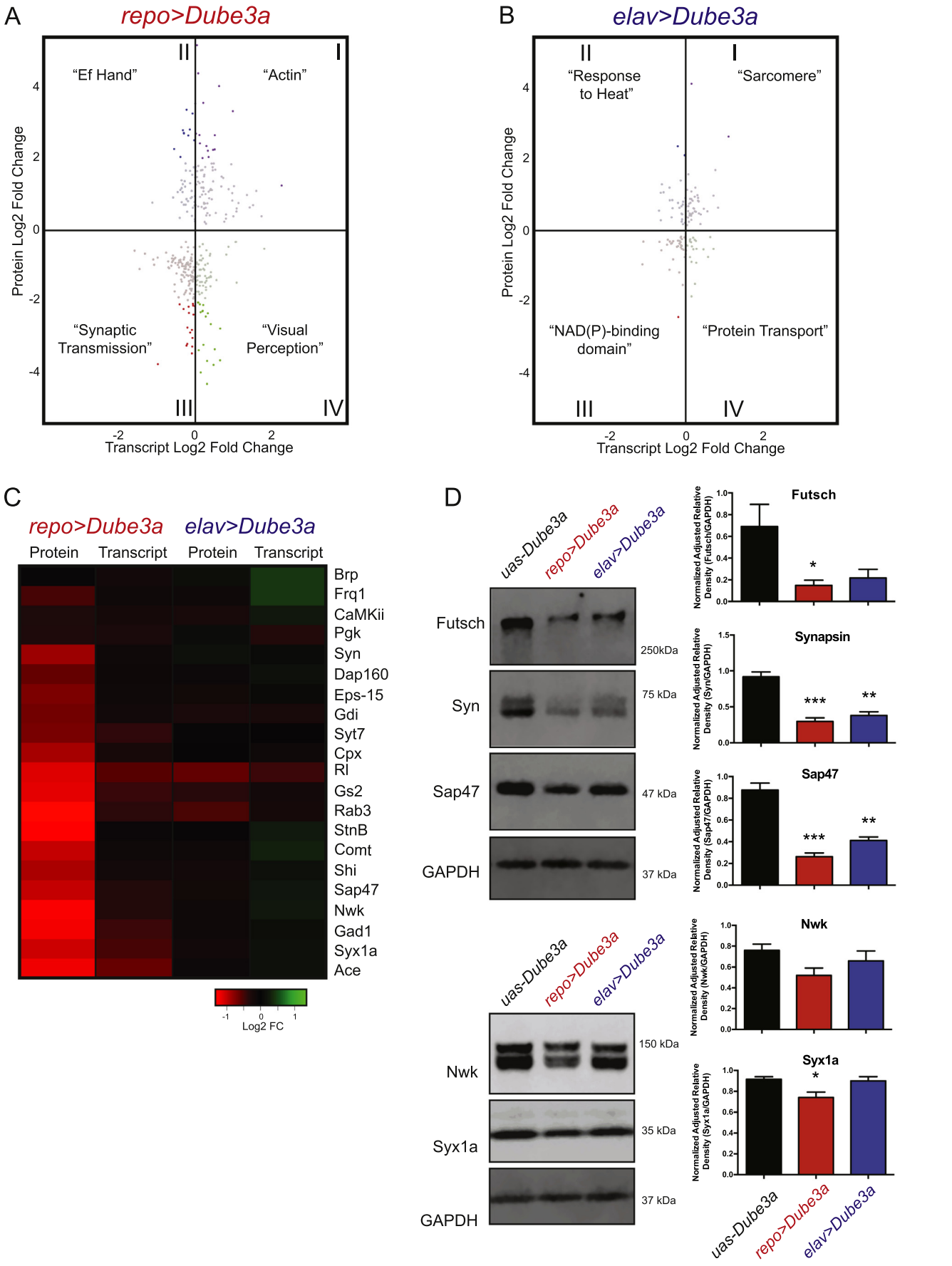

(caption on next page)

Fig. 3. Cell non-autonomous downregulation of synaptic transmission proteins in *repo > Dube3a* flies. A) Log_2 fold change of significantly differentially expressed proteins also detected at the transcript and protein level in *repo > Dube3a* and B) Log_2 fold change of significantly differentially expressed proteins also detected at the transcript level. The top DAVID enrichment group is stated in each quadrant of the graph. C) Heatmap of genes at the transcript and protein level for the "synaptic transmission" enrichment group in both *repo > Dube3a* and *elav > Dube3a*. Note the cell non-autonomous downregulation observed for neuronal proteins in *repo > Dube3a* brain. D) Quantitative IR western blot confirmation of "synaptic transmission" protein downregulation in both *repo > Dube3a* and *elav > Dube3a*. N ≥ 3 for each genotype, error bars represent S.E.M., and * = p ≤ 0.05, ** = p ≤ 0.01, and *** = p ≤ 0.005.

upregulated at the transcript level (Fig. 3A).

In *elav > Dube3a*, 67 of the 81 upregulated proteins (82.3%) were differentially expressed at the transcript level. In quadrant I, 40 of these 67 upregulated proteins (59.7%) were also upregulated at the transcript level, while in quadrant II, 27 (40.3%) of upregulated proteins were downregulated at the transcript level. Of the 56 downregulated proteins in *elav > Dube3a*, all 56 genes (100%) were also differentially expressed at the transcript level. Quadrant III included 33 of the 56 (58.9%) downregulated proteins that were also downregulated at the transcript level. Quadrant IV included 23 of 56 (41.1%) downregulated proteins that were upregulated at the transcript level (Fig. 3B). Combining both *repo > Dube3a* and *elav > Dube3a* datasets for genes in which we detected significant expression differences at both the transcript and protein level, we observed a concordance of 60.7% for genes changing both transcript and protein levels in the same direction.

In quadrant III of *repo > Dube3a* we observed a significant DAVID enrichment in the GO term "synaptic transmission" (Enrichment Score = 15.7). This enrichment included 21 genes, and we plotted Log_2 fold change values for each gene at the protein and transcript level in both *repo > Dube3a* and *elav > Dube3a* (Fig. 3C) all of which are downregulated in *repo > Dube3a* but relatively unchanged in *elav > Dube3a* flies. These data suggest cell non-autonomous effects of *Dube3a* overexpression in glia, whereby glial elevation of Dube3a causes downregulation of neuronal synaptic transmission proteins.

Next, we tried to validate the downregulation of synaptic proteins observed through RNAseq and proteomics via western blot (Fig. 3D). We observed a significant effect of genotype on synapsin levels (One-way ANOVA, n = 3, p ≤ 0.005), a vesicle protein that regulates neurotransmitter release (Winther et al., 2015), and found that synapsin is downregulated at the protein level in *repo > Dube3a* compared to control *uas-Dube3a* flies (Tukey's multiple comparisons; p ≤ 0.005). We found a downregulation of synapsin in *elav > Dube3a* compared to *uas-Dube3a* flies (Tukey's multiple comparisons; p ≤ 0.01) that was not detected during our proteomic analysis. In addition to synapsin, we confirmed the downregulation of Sap47, a vesicle associated protein (Saumweber et al., 2011), at the protein level with genotype displaying a significant effect on Sap47 levels (One-way ANOVA, n = 3, p ≤ 0.005). We observed reduced Sap47 levels in *repo > Dube3a* compared to *uas-Dube3a* flies (Tukey's multiple comparisons; p ≤ 0.005) and in *elav > Dube3a* flies (Tukey's multiple comparisons; p ≤ 0.005). Although not included in our analysis comparing the proteome and transcriptome, because *futsch* was not detected at the transcript level, we tested levels of the neuronal microtubule protein futsch and detected a significant downregulation of futsch protein levels in *repo > Dube3a* compared to *uas-Dube3a* alone (One-way ANOVA, n = 3, p ≤ 0.05, Tukey's multiple comparisons; p ≤ 0.05). Syx1a mediates vesicle fusion (Schulze et al., 1995), and Syx1a protein expression was also dependent upon genotype (One-way ANOVA, n = 8, p ≤ 0.05), and levels were significantly reduced only in *repo > Dube3a* compared to *uas-Dube3a* controls (Tukey's multiple comparisons, n = 8, p ≤ 0.05). We also tested levels of Nwk, a protein that regulates synapse morphology and actin dynamics (Rodal et al., 2008), however there was slightly more variation and no significant differences were detected between genotypes (One-way ANOVA; p = 0.11). Validating the downregulation of five synaptic proteins by Western blot supports the results from our proteomics dataset. These data suggest that synaptic proteins may be downregulated in *repo > Dube3a* flies in a cell non-autonomous manner, as we are manipulating *Dube3a* expression in glial cells.

3.4. Glutathione S-transferase upregulation is common among gliopathic seizure flies

We wanted to know whether any of the molecular changes that occur in our Dup15q fly model of epilepsy were common to other epilepsies studied in flies and if these "bang sensitive" genes could cause seizures when manipulated in glial cells. We identified and selected 54 different UAS lines that covered 34 genes which were associated with the term "bang sensitive" in FlyBase. We crossed these uas-RNAi or uas-cDNA lines to *repo*-GAL4 to manipulate gene expression within glial cells. We found lethality in 6 of these lines (Supplemental Table 7) and identified 6 additional lines that cause a bang sensitive seizure phenotype when crossed to *repo*-GAL4 (Fig. 4A, One-Way ANOVA, p ≤ 0.0001; Dunnett's multiple comparison test p ≤ 0.05; see Supplemental Table 1 for all lines tested). We called these flies "gliopathic" seizure flies because they have seizures driven by glial cell manipulations, most of which were RNAi knockdown of endogenous glial genes. We collected total head mRNA from 5 of these gliopathic lines along with *repo > Dube3a*, pooled them to one group, and performed an mRNA microarray analysis to look for shared transcriptional changes among all of the lines (*repo > COX7A-RNAi* was excluded from the microarray due to a less severe seizure phenotype, however it was included in subsequent qRT-PCR analysis). Upon comparing the gliopathic seizure group to a *repo > 36303-emptyvector-RNAi* control line, we observed 120 significantly differentially expressed transcripts (FDR ≤ 0.05, Supplemental Table 8). DAVID analysis of these differentially expressed genes revealed a significant enrichment in the GO term "Detoxification" (ES = 2.45), comprising the GSTs *GSTD2*, *GSTD5*, and *GSTS1*. Additionally, we observed an enrichment in "glutathione S-transferase activity" (ES = 2.31), including the additional gene *GSTE7* (Supplemental Table 8). Gene expression studies for *GSTS1*, *GSTD2*, *GSTE7*, and *GSTD5* on each individual line, confirmed an upregulation of these GST transcripts in 5 out of the 7 gliopathic seizure lines (Fig. 4B). These data indicate that GST upregulation is a common occurrence in gliopathic seizure and is not a phenomenon specific to our fly model of Dup15q epilepsy.

To determine whether the upregulation of GSTs occurred cell autonomously within glia or non-autonomously within another cell type in the brain, such as neurons, we used a previously published *GSTD1-LacZ* reporter line (Sykiotis and Bohmann, 2008). In control *repo*-GAL4;*GSTD1-LacZ* flies staining for α-βGal was relatively diffuse (Fig. 4C, top row). However, in *repo > Dube3a;GSTD1-LacZ* seizure flies we observed a marked increase in α-βGal immunoreactivity which colocalized strongly with the glial-specific transcription factor *repo* (Fig. 4C, bottom row). We quantified LacZ fluorescence in the area surrounding $Repo^+$ glial cell nuclei in control (1518.00 ± 563.36 A.U., mean ± SD, N = 10 cells) and *Dube3a* overexpression brains (4514.73 ± 2270.3 A.U., N = 10 cells), and identified a statistically significant increase in GSTD1-LacZ signal in *repo > Dube3a;GSTD1-LacZ* flies (2-tailed *t*-test, p ≤ 0.01). Finally, we asked whether inducing seizure-like activity alone through pharmacological means would similarly result in GST upregulation. We fed *GSTD1-LacZ* flies 2.5 mM picrotoxin (PTX) or DMSO (control) overnight to induce seizure-like behavior, and upregulation of *GSTD1-LacZ* did not occur in PTX fed flies (Supplemental Figure 1). Taken together, these data suggest that GST upregulation is common among gliopathic seizure flies and occurs cell

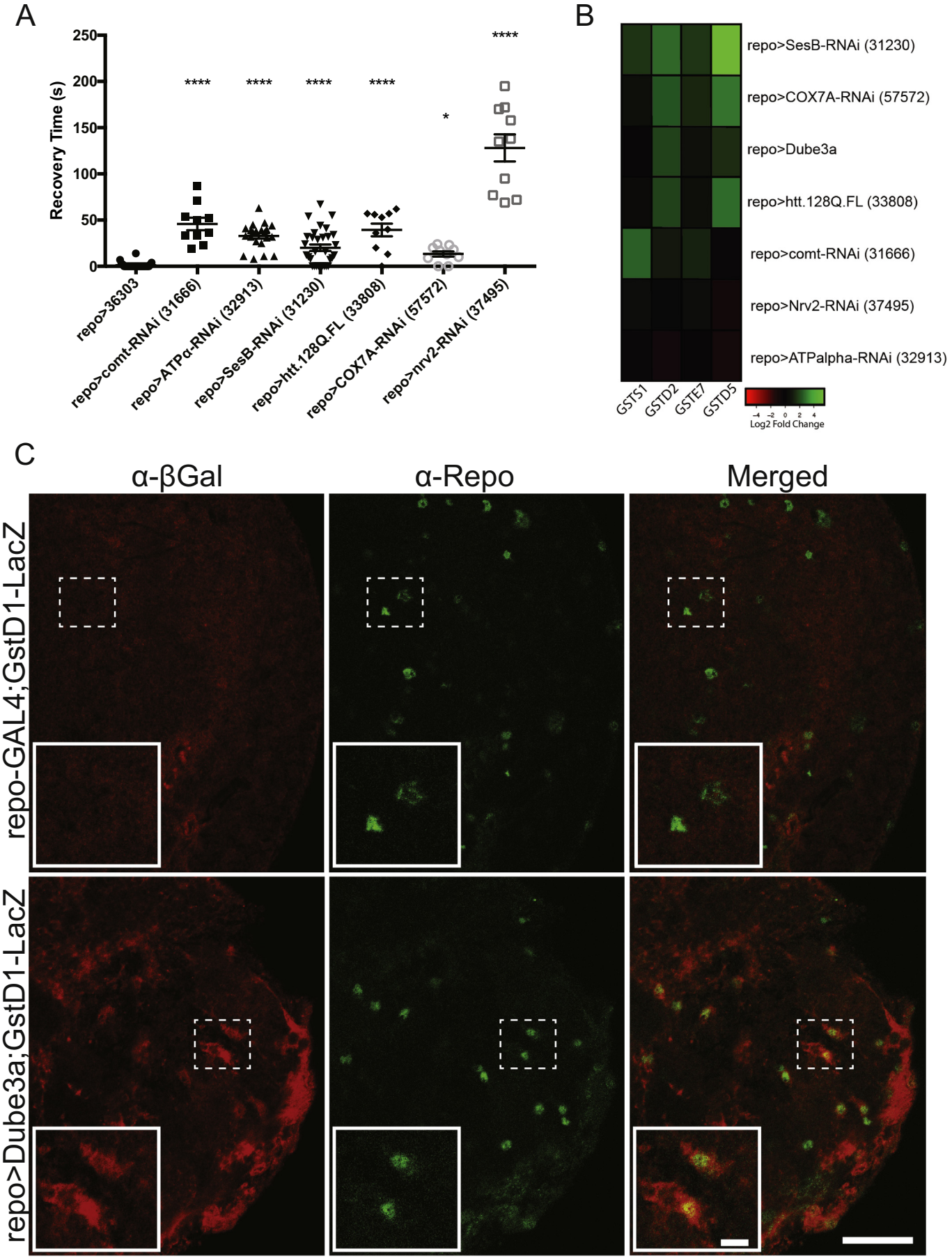

(caption on next page)

Fig. 4. Glutathione S-transferase upregulation is common among multiple "gliopathic" seizure lines and occurs cell autonomously within glial cells. A) Recovery times in the bang sensitivity seizure assay for 6 additional gliopathic seizure lines identified ($p \leq 0.05$ compared to *repo > 36303*). B) Heatmap of glutathione S-transferase expression levels in each gliopathic seizure line indicates upregulation of glutathione S-transferases in 5/7 lines. Genes were originally identified by microarray as differentially expressed in a pooled gliopathic seizure group compared to a control group. C) Immunohistochemistry in *repo-GAL4;GstD1-LacZ* or *repo > Dube3a;GstD1-LacZ* for the glutathione S-transferase reporter GstD1-LacZ reveals an upregulation of glutathione S-transferases cell autonomously within glial cells. All glial cells are marked with an α-repo antibody. Error bars represent S.E.M. and scale bars represent 25 μm or 5 μm (inset).

autonomously within glial cells.

4. Discussion

In this study we show that glial *Dube3a* overexpression causes downregulation of synaptic transmission genes at the transcript and protein levels. We also demonstrate a cell autonomous upregulation of GSTs that was shared among multiple gliopathic seizure lines that we identified. In contrast, *Dube3a* overexpression in neurons resulted in fewer overall changes in the transcriptome and proteome, and fewer biologically relevant enrichment groups compared to *Dube3a* overexpression in glia. This study demonstrates the utility of Drosophila for identifying global changes in the transcriptome and proteome depending on the cell type overexpressing *Dube3a* (glia or neurons). We went on to show shared molecular changes across multiple genes causing gliopathic seizure.

Our proteomic experiments identified a sizeable portion of the Drosophila head proteome. While not exhaustive, we reliably measured peptides corresponding to 2,503 proteins. Recent efforts to completely identify the Drosophila head proteome revealed peptides corresponding to 4,559 proteins (Aradska et al., 2015). Despite the lower coverage, we observed synaptic transmission protein downregulation in *repo > Dube3a* flies which we confirmed via western blot. Importantly, these experiments were not designed to detect direct ubiquitin ligase substrates of Dube3a, only the consequences of *Dube3a* overexpression in different cell types. As such, the changes observed at the protein level could be secondary, tertiary, or even quaternary effects due to *Dube3a* overexpression. We observed an enrichment of downregulated proteins in the gene ontology term "synaptic transmission" in *repo > Dube3a* flies, suggesting cell non-autonomous effects of *Dube3a* overexpression in glia. Some of these genes are expressed in glia and contribute to the synaptic transmission process, such as *glutamine synthetase 2* (*Gs2*) which converts glutamate to glutamine (Sinakevitch et al., 2010). However, genes including *futsch* (Hummel et al., 2000), *synapsin* (Oland et al., 2008), *Sap47* (Saumweber et al., 2011; Reichmuth et al., 1995), *bruchpilot* (Wagh et al., 2006), and *nervous wreck* (Rodal et al., 2008) are predominantly expressed in neurons. Therefore, our results show that *repo > Dube3a* has a cell non-autonomous effect on gene expression in neurons.

Human orthologs of some of the synaptic transmission proteins downregulated in *repo > Dube3a* flies are associated with human epilepsy. Nonsense variants in *Synapsin I*, the human ortholog of Drosophila *synapsin*, were identified in two separate families segregating epilepsy and in an ASD/epilepsy cohort (Garcia et al., 2004; Fassio et al., 2011). Drosophila *Syx1a* is orthologous to human *STX1B*, and mutations in *STX1B* are associated with febrile seizures and epilepsy (Schubert et al., 2014). The data from our fly model suggests these proteins may be implicated in Dup15q epilepsy, and alterations in these synaptic proteins in the Dup15q brain remain to be explored.

Glial GST upregulation may broadly underlie treatment resistant epilepsies. GSTs are upregulated in the human brain in cases of treatment resistant epilepsy, particularly in astrocytes surrounding blood vessels (Shang et al., 2008). While the factor initiating GST upregulation in seizure remains unknown, we show here that chemical induction of seizure activity did not result in GST up regulation, implying the neuronal activity alone is not the cause. GST upregulation occurred within glia in response to oxidative stress in a fly model of Alexander disease (Wang et al., 2011; Wang et al., 2016) and in a mammalian *in vitro* culture system during increased neuronal activity (McGann and Mandel, 2018). One hypothesis surrounding GSTs in treatment resistant epilepsy is glia of the blood brain barrier upregulate GSTs, whether from oxidative stress or increased neuronal activity during seizure, causing antiepileptic drug metabolism before they enter the brain. Indeed, in cancer, GST upregulation is associated with increased drug metabolism and chemoresistance (Sau et al., 2010; Allocati et al., 2018), suggesting GST upregulation as a cause of treatment resistant epilepsy as well.

While this study clearly demonstrates that glial cells upregulate GSTs in gliopathic seizures, it remains unclear whether the upregulation of GSTs is a cause of seizure or an effect from seizure. One possibility is that glial GST upregulation is sufficient to trigger seizure activity. Alternatively, glia may upregulate GSTs as a response to prevent seizures, or to mitigate cellular damage resulting from seizures. Future experiments will focus on distinguishing these two possibilities in order to determine the role (harmful or protective) of GSTs in epilepsy.

These data suggest that in addition to GST upregulation, glial cell dysfunction itself causes at least some epileptic pathologies. Glial-specific knockdown of mitochondrial related genes *COX7A* or *SesB* resulted in seizure phenotypes, and mitochondrial dysfunction has been proposed as a cause of epilepsy (Khurana et al., 2013). Additionally, glial-specific knockdown of *comatose* (*comt*), the gene encoding N-ethylmaleimide-sensitive factor 1, caused bang-sensitive seizures. Vesicle release machinery and exocytosis occurs in astrocytes (Reviewed in Vardjan et al., 2016). Our findings suggest that altering vesicle function may also result in seizure susceptibility.

In conclusion, we found cell non-autonomous downregulation of synaptic transmission proteins in *repo > Dube3a* flies combined with GST upregulation not only in Dup15q related *repo > Dube3a* animals but across gliopathic epilepsies we tested. Our results highlight the use of Drosophila for investigating cell-type specific genetic manipulations and provides novel avenues to investigate in Dup15q and treatment resistant epilepsy.

Supplementary data to this article can be found online at https://doi.org/10.1016/j.nbd.2020.104879.

Author credit statement

KH designed experiments, executed experiments, performed data analysis and wrote the manuscript; DJ and PWM assisted in bioinformatic analysis; DLF provided proteomics support; DK ran proteomics samples and LTR provided funding, directed these studies and assisted in writing the manuscript.

Declaration of Competing Interest

None.

Acknowledgements

This work was supported in part by a pre-doctoral fellowship from the Duplication 15q Alliance to KAH and an NICHD grant to LTR (NIH R21HD091541). We also acknowledge the use of stocks from the Bloomington Drosophila Stock Center (NIH P40OD018537) and antibodies from the Developmental Studies Hybridoma Bank at the University of Iowa, created by the NICHD.

References

Allocati, N., Masulli, M., Di Ilio, C., Federici, L., 2018. Glutathione transferases: substrates, inihibitors and pro-drugs in cancer and neurodegenerative diseases. Oncogenesis 7, 8.

Aradska, J., Bulat, T., Sialana, F.J., Birner-Gruenberger, R., Erich, B., Lubec, G., 2015. Gel-free mass spectrometry analysis of Drosophila melanogaster heads. Proteomics 15, 3356–3360.

Brand, A.H., Perrimon, N., 1993. Targeted gene expression as a means of altering cell fates and generating dominant phenotypes. Development 118, 401–415.

Burette, A.C., Judson, M.C., Li, A.N., Chang, E.F., Seeley, W.W., Philpot, B.D., Weinberg, R.J., 2018. Subcellular organization of UBE3A in human cerebral cortex. Mol. Autism 9, 54.

Conant, K.D., Finucane, B., Cleary, N., Martin, A., Muss, C., Delany, M., Murphy, E.K., Rabe, O., Luchsinger, K., Spence, S.J., et al., 2014. A survey of seizures and current treatments in 15q duplication syndrome. Epilepsia 55, 396–402.

Copping, N., Christian, S., Ritter, D., Islam, M., Buscher, N., Zolkowska, D., Pride, M., Berg, E., LaSalle, J., Ellegood, J., et al., 2017. Neuronal overexpression of Ube3a isoform 2 causes behavioral impairments and neuroanatomical pathology relevant to 15q11.2-q13.3 duplication syndrome. Hum. Mol. Genet. 26 (20), 3995–4010.

Coulter, D.A., Steinhauser, C., 2015. Role of astrocytes in epilepsy. Cold Spring Harb. Perspect. Med. 5, a022434.

Dindot, S.V., Antalffy, B.A., Bhattacharjee, M.B., Beaudet, A.L., 2008. The Angelman syndrome ubiquitin ligase localizes to the synapse and nucleus, and maternal deficiency results in abnormal dendritic spine morphology. Hum. Mol. Genet. 17, 111–118.

Duffy, J.B., 2002. GAL4 system in Drosophila: a fly geneticist's Swiss army knife. Genesis 34, 1–15.

Fassio, A., Patry, L., Congia, S., Onofri, F., Piton, A., Gauthier, J., Pozzi, D., Messa, M., Defranchi, E., Fadda, M., et al., 2011. SYN1 loss-of-function mutations in autism and partial epilepsy cause impaired synaptic function. Hum. Mol. Genet. 20, 2297–2307.

Fiest, K.M., Sauro, K.M., Wiebe, S., Patten, S.B., Kwon, C.S., Dykeman, J., Pringsheim, T., Lorenzetti, D.L., Jette, N., 2017. Prevalence and incidence of epilepsy: A systematic review and meta-analysis of international studies. Neurology 88, 296–303.

Finucane, B.M., Lusk, L., Arkilo, D., Chamberlain, S., Devinsky, O., Dindot, S., Jeste, S.S., LaSalle, J.M., Reiter, L.T., Schanen, N.C. *et al.* (2016) In Pagon, R. A., Adam, M. P., Ardinger, H. H., Wallace, S. E., Amemiya, A., Bean, L. J. H., Bird, T. D., Ledbetter, N., Mefford, H. C., Smith, R. J. H. *et al.* (eds.), GeneReviews(R), Seattle (WA).

Garcia, C.C., Blair, H.J., Seager, M., Coulthard, A., Tennant, S., Buddles, M., Curtis, A., Goodship, J.A., 2004. Identification of a mutation in synapsin I, a synaptic vesicle protein, in a family with epilepsy. J. Med. Genet. 41, 183–186.

Golyala, A., Kwan, P., 2017. Drug development for refractory epilepsy: The past 25 years and beyond. Seizure 44, 147–156.

Grier, M.D., Carson, R.P., Lagrange, A.H., 2015. Toward a broader view of Ube3a in a mouse model of Angelman syndrome: expression in brain, spinal cord, sciatic nerve and glial cells. PLoS One 10, e0124649.

Hope, K.A., LeDoux, M.S., Reiter, L.T., 2017. Glial overexpression of Dube3a causes seizures and synaptic impairments in Drosophila concomitant with down regulation of the Na+/K+ pump ATPalpha. Neurobiol. Dis. 108, 238–248.

Huang Da, W., Sherman, B.T., Lempicki, R.A., 2009a. Bioinformatics enrichment tools: paths toward the comprehensive functional analysis of large gene lists. Nucleic Acids Res. 37, 1–13.

Huang Da, W., Sherman, B.T., Lempicki, R.A., 2009b. Systematic and integrative analysis of large gene lists using DAVID bioinformatics resources. Nat. Protoc. 4, 44–57.

Hummel, T., Krukkert, K., Roos, J., Davis, G., Klambt, C., 2000. Drosophila Futsch/22C10 is a MAP1B-like protein required for dendritic and axonal development. Neuron 26, 357–370.

Jensen, L., Farook, M.F., Reiter, L.T., 2013. Proteomic profiling in Drosophila reveals potential Dube3a regulation of the actin cytoskeleton and neuronal homeostasis. PLoS One 8, e61952.

Jiang, X., Bomgarden, R., Brown, J., Drew, D.L., Robitaille, A.M., Viner, R., Huhmer, A.R., 2017. Sensitive and Accurate Quantitation of Phosphopeptides Using TMT Isobaric Labeling Technique. J. Proteome Res. 16, 4244–4252.

Judson, M.C., Sosa-Pagan, J.O., Del Cid, W.A., Han, J.E., Philpot, B.D., 2014. Allelic specificity of Ube3a expression in the mouse brain during postnatal development. J. Comp. Neurol. 522, 1874–1896.

Khurana, D.S., Valencia, I., Goldenthal, M.J., Legido, A., 2013. Mitochondrial dysfunction in epilepsy. Semin. Pediatr. Neurol. 20, 176–187.

Krishnan, V., Stoppel, D.C., Nong, Y., Johnson, M.A., Nadler, M.J., Ozkaynak, E., Teng, B.L., Nagakura, I., Mohammad, F., Silva, M.A., et al., 2017. Autism gene Ube3a and seizures impair sociability by repressing VTA Cbln1. Nature 543, 507–512.

Kwan, P., Brodie, M.J., 2000. Early identification of refractory epilepsy. N. Engl. J. Med. 342, 314–319.

LaPenna, P., Tormoehlen, L.M., 2017. The Pharmacology and Toxicology of Third-Generation Anticonvulsant Drugs. J Med Toxicol 13, 329–342.

LaSalle, J.M., Reiter, L.T., Chamberlain, S.J., 2015. Epigenetic regulation of UBE3A and roles in human neurodevelopmental disorders. Epigenomics 7, 1213–1228.

Lee, S.Y., Ramirez, J., Franco, M., Lectez, B., Gonzalez, M., Barrio, R., Mayor, U., 2014. Ube3a, the E3 ubiquitin ligase causing Angelman syndrome and linked to autism, regulates protein homeostasis through the proteasomal shuttle Rpn10. Cell. Mol. Life Sci. 71, 2747–2758.

McGann, J.C., Mandel, G., 2018. Neuronal activity induces glutathione metabolism gene expression in astrocytes. Glia 66, 2024–2039.

Nakatani, J., Tamada, K., Hatanaka, F., Ise, S., Ohta, H., Inoue, K., Tomonaga, S., Watanabe, Y., Chung, Y.J., Banerjee, R., et al., 2009. Abnormal behavior in a chromosome-engineered mouse model for human 15q11-13 duplication seen in autism. Cell 137, 1235–1246.

Oland, L.A., Biebelhausen, J.P., Tolbert, L.P., 2008. Glial investment of the adult and developing antennal lobe of Drosophila. J. Comp. Neurol. 509, 526–550.

Reichmuth, C., Becker, S., Benz, M., Debel, K., Reisch, D., Heimbeck, G., Hofbauer, A., Klagges, B., Pflugfelder, G.O., Buchner, E., 1995. The sap47 gene of Drosophila melanogaster codes for a novel conserved neuronal protein associated with synaptic terminals. Brain Res. Mol. Brain Res. 32, 45–54.

Reiter, L.T., Seagroves, T.N., Bowers, M., Bier, E., 2006. Expression of the Rho-GEF Pbl/ECT2 is regulated by the UBE3A E3 ubiquitin ligase. Hum. Mol. Genet. 15, 2825–2835.

Rodal, A.A., Motola-Barnes, R.N., Littleton, J.T., 2008. Nervous wreck and Cdc42 cooperate to regulate endocytic actin assembly during synaptic growth. J. Neurosci. 28, 8316–8325.

Sau, A., Pellizzari Tregno, F., Valentino, F., Federici, G., Caccuri, A.M., 2010. Glutathione transferases and development of new principles to overcome drug resistance. Arch. Biochem. Biophys. 500, 116–122.

Saumweber, T., Weyhersmuller, A., Hallermann, S., Diegelmann, S., Michels, B., Bucher, D., Funk, N., Reisch, D., Krohne, G., Wegener, S., et al., 2011. Behavioral and synaptic plasticity are impaired upon lack of the synaptic protein SAP47. J. Neurosci. 31, 3508–3518.

Schindelin, J., Arganda-Carreras, I., Frise, E., Kaynig, V., Longair, M., Pietzsch, T., Preibisch, S., Rueden, C., Saalfeld, S., Schmid, B., et al., 2012. Fiji: an open-source platform for biological-image analysis. Nat. Methods 9, 676–682.

Schubert, J., Siekierska, A., Langlois, M., May, P., Huneau, C., Becker, F., Muhle, H., Suls, A., Lemke, J.R., de Kovel, C.G., et al., 2014. Mutations in STX1B, encoding a presynaptic protein, cause fever-associated epilepsy syndromes. Nat. Genet. 46, 1327–1332.

Schulze, K.L., Broadie, K., Perin, M.S., Bellen, H.J., 1995. Genetic and electrophysiological studies of Drosophila syntaxin-1A demonstrate its role in nonneuronal secretion and neurotransmission. Cell 80, 311–320.

Shang, W., Liu, W.H., Zhao, X.H., Sun, Q.J., Bi, J.Z., Chi, Z.F., 2008. Expressions of glutathione S-transferase alpha, mu, and pi in brains of medically intractable epileptic patients. BMC Neurosci. 9, 67.

Sinakevitch, I., Grau, Y., Strausfeld, N.J., Birman, S., 2010. Dynamics of glutamatergic signaling in the mushroom body of young adult Drosophila. Neural Dev. 5, 10.

Smith, S.E., Zhou, Y.D., Zhang, G., Jin, Z., Stoppel, D.C., Anderson, M.P., 2011. Increased gene dosage of Ube3a results in autism traits and decreased glutamate synaptic transmission in mice. Sci Transl Med 3 103ra197.

Sykiotis, G.P., Bohmann, D., 2008. Keap1/Nrf2 signaling regulates oxidative stress tolerance and lifespan in Drosophila. Dev. Cell 14, 76–85.

Vardjan, N., Parpura, V., Zorec, R., 2016. Loose excitation-secretion coupling in astrocytes. Glia 64, 655–667.

Wagh, D.A., Rasse, T.M., Asan, E., Hofbauer, A., Schwenkert, I., Durrbeck, H., Buchner, S., Dabauvalle, M.C., Schmidt, M., Qin, G., et al., 2006. Bruchpilot, a protein with homology to ELKS/CAST, is required for structural integrity and function of synaptic active zones in Drosophila. Neuron 49, 833–844.

Wang, L., Colodner, K.J., Feany, M.B., 2011. Protein misfolding and oxidative stress promote glial-mediated neurodegeneration in an Alexander disease model. J. Neurosci. 31, 2868–2877.

Wang, L., Hagemann, T.L., Messing, A., Feany, M.B., 2016. An in vivo pharmacological screen identifies cholinergic signaling as a therapeutic target in glial-based nervous system disease. J. Neurosci. 36, 1445–1455.

Winther, A.M., Vorontsova, O., Rees, K.A., Nareoja, T., Sopova, E., Jiao, W., Shupliakov, O., 2015. An endocytic scaffolding protein together with synapsin regulates synaptic vesicle clustering in the drosophila neuromuscular junction. J. Neurosci. 35, 14756–14770.

Yamasaki, K., Joh, K., Ohta, T., Masuzaki, H., Ishimaru, T., Mukai, T., Niikawa, N., Ogawa, M., Wagstaff, J., Kishino, T., 2003. Neurons but not glial cells show reciprocal imprinting of sense and antisense transcripts of Ube3a. Hum. Mol. Genet. 12, 837–847.